



LIGHT CURVE CHARACTERISTICS OF GAMMA-RAY BURSTS

By

Temam Beyan

**A THESIS SUBMITTED TO
GRADUATE PROGRAMS OF
ADDIS ABABA UNIVERSITY
IN PARTIAL FULFILLMENT FOR THE REQUIREMENTS
OF THE DEGREE
MASTER OF SCIENCE IN PHYSICS
(ASTRONOMY/ASTROPHYSICS)
ADDIS ABABA, ETHIOPIA
AUGUST 2022**

ADDIS ABABA UNIVERSITY
PROGRAM OF GRADUATE STUDIES

LIGHT CURVE CHARACTERISTICS OF GAMMA-RAY BURSTS

By
Temam Beyan
Department of Physics
Addis Ababa University

Approved by the Examining Board:

Dr. Firaol Fana
Advisor

Signature

Examiner

Signature

Examiner

Signature

Date: August 2022

ADDIS ABABA UNIVERSITY

Date: **August 2022**

Author: **Temam Beyan**

Title: **Light Curve Charactersics Of Gamma-Ray Bursts**

Department: **Department of Physics**

Degree: **M.Sc.** Convocation: **April** Year: **2021**

Permission is herewith granted to Addis Ababa University to circulate and to have copied for non-commercial purposes, at its discretion, the above title upon the request of individuals or institutions.

Signature of Author

THE AUTHOR RESERVES OTHER PUBLICATION RIGHTS, AND NEITHER THE THESIS NOR EXTENSIVE EXTRACTS FROM IT MAY BE PRINTED OR OTHERWISE REPRODUCED WITHOUT THE AUTHOR'S WRITTEN PERMISSION.

THE AUTHOR ATTESTS THAT PERMISSION HAS BEEN OBTAINED FOR THE USE OF ANY COPYRIGHTED MATERIAL APPEARING IN THIS THESIS (OTHER THAN BRIEF EXCERPTS REQUIRING ONLY PROPER ACKNOWLEDGEMENT IN SCHOLARLY WRITING) AND THAT ALL SUCH USE IS CLEARLY ACKNOWLEDGED.

This Work is Dedicated

to

*My brothers Mulugeta Asfie and Kalamlak Azanaw died
in 1995 / 1997 E.C*

Table of Contents

Table of Contents	v
List of Table	viii
List of Figures	ix
Acknowledgements	xi
Abbreviations	xii
Physical Constants	xiii
Symbols	xiv
Abstract	xv
1 Physics of gamma-ray bursts.	1
1.1 Introduction	1
1.2 Historical Discovery of gamma-Ray bursts	2
1.2.1 Dark era (1967-1990)	2
1.2.2 BATSE era (1991-2000)	4
1.2.3 BeppoSAX era (1997-2000)	5
1.2.4 Swift era(2004-now)	6
1.2.5 Fermi era (2008-now)	7
1.3 Classification of gamma-ray bursts	8
1.3.1 short/hard gamma-ray bursts	8
1.3.2 long/soft gamma-ray bursts	9
1.3.3 Ultra long gamma-ray bursts (ULGRBs)	9
1.4 Global properties of GRBs	10
1.4.1 Intensity distribution	10
1.4.2 Angular distribution	11
1.5 Statement of the problems	11

1.6	Objectives and thesis outline	12
2	Emission mechanisms and observational properties of gamma-ray bursts	13
2.1	Introduction	13
2.2	GRBs production mechanisms	13
2.2.1	Basic fireball model	14
2.2.2	progenitors of GRBs	20
2.2.3	Working mechanisms of central engine	20
2.2.4	GRB-SN association	21
2.3	GRBs Obsevation and interpretations	21
2.3.1	prompt GRB emission	21
2.3.2	Afterglow GRB emission	23
2.4	Interpretations of GRBs afterglow	24
2.4.1	Early time afterglow	25
2.4.2	Late time afterglow	25
2.5	Theoritical interpretation of X-ray afterglow	25
2.5.1	steep decay of early X-ray light curves	26
2.5.2	Shallow /plateau decay X-ray light curves	27
2.5.3	normal decay phase	27
2.5.4	Late steep decay following the plateau in X-ray light curves .	28
2.5.5	Time breaks in swift X-ray afterglow	28
2.5.6	The first break in the light curve ($t_{break,1}$)	28
2.6	Decay of flux with time of observed light currve	29
2.7	calculating luminosity (L) of x-ray afterglow	31
3	Research methodology	33
3.1	Research designs	33
3.2	Data sources,sampling techniques and size	34
3.2.1	Data sources and types.	34
3.2.2	Data sampling technique and size	34
3.3	Validity and reliability of data	34
3.4	processing and analyzing data	34
3.5	Evaluating and justifying methodology	34
4	Result And Discussion	35
4.1	Introduction	35

5 Conclusion	36
Bibliography	37

List of Tables

List of Figures

1.1	Light curve of the first GRB ever detected by Vela. Two separate pulses can be identified over a duration of less than 10 seconds [4] .	3
1.2	The distribution of all 2704 GRBs detected by BATSE satellite: they are clearly isotropically distributed [7].	4
1.3	Schematic view of the swift satellite(Gehrels et.al 2004).The size of Mask of BAT is $2.7m^2$ [7]	6
1.4	The GRB classification (long and short) distribution.	8
2.1	Visualisation of the fireball model (from Gehrels et al. (2002), credit Juan Velasco)[13]	16
2.2	Standard fireball model.	17
2.3	Qualitative schematic view of the structure of the relativistic jet produced by the gamma-ray burst. The external shock arises as a result of the impact of the jet on the stellar wind of the progenitor. This is where the final goodbye of the SOS similar emission from the collapsing star forms, which is characterized by a smooth (but non-monotonic) light variation. The internal shock persists as long as the central engine continues operating this is where rapidly varying gamma-, x-ray, and optical radiation forms.	18
2.4	Schematic evolution of the jet Lorentz factor and examples of symbolic locations of radius: the saturation radius r_s , photospheric radius r_{ph} , internal shock radius r_{is} and external shock r_{es}	22
2.5	Diverse light curves of the GRBs prompt emission detected by BATSE instrument.This sample includes short and long events. https://gammaray.nsstc.nasa.gov	

2.6	Canonical GRB light curve. The prompt phase is often followed by a steep decay phase (typical index of 3) which can then break to a shallower decline (shallow decay phase), a standard afterglow phase (pre-jet break phase), and possibly, a jet break and post-jet break phase. Sometimes an X-ray flare is seen.	26
2.7	A sketch of the various angles and distances for the large angle (or high latitude) emission when the γ -ray source turns off suddenly. . .	29

Acknowledgements

First of all, I thanks to God for His unlimited love, care, and undesirable help He has done to me throughout my life. I would like to express my deep gratitude to my advisor and instructor Dr. Remudin Reshid for his continuous guidance and great support. I would like to extend my thanks to my instructors and the department of physics of the Addis Ababa University and its staffs, I have learned many things from them like respecting teaching profession, punctuality, encouraging learners to have creative mind and so on. I would also like to acknowledge the financial support for my studies provided by the Addis Ababa Educational Bureau. Finally, I am very grateful thanks to my friends Murad Yimam, Debela Alemayehu, Jemal Regassa, Natnael and all my classmates I have received many comments and feed backs.

Addis Ababa University

Temam Beyan

April, 2021

Abbreviations

ASD	Amplitude Spectral Density
AXPs	Anomalous X-Ray Pulsars
EFE	Einstein Field Equation
BBH	Binary Black hole
BBN	Big Bang Nucleosynthesis
BHNS	Black hole Neutron Star
CBC	Compact Binary Coalescence
CMBR	Cosmic Microwave Background Radiation
CW	Continuous Wave
PN	Post Newtonian
GRBs	Gama-ray Bursts
GR	General Relativity
GW	Gravitational Wave
LIGO	Laser Interferometer Gravitational Wave Observatory
LISA	Laser Interferometer Space Astronomy
MBH	Massive Black hole
NR	Numerical Relativity
SEOBNR	Spin Effective One Body Numerical Relativity
IMRPhenom	In-spiral Merge Ringdown Phenomenological
PSDs	Power Spectral Density
SGRS	Soft Gama-ray Repeaters
SNR	Signal to Noise Ratio

Physical Constants

Speed of Light	$C = 2.99792458 \times 10^8 \text{ ms}^{-2}$
Universal Gravitational Constant	$G = 6.67 \times 10^{-11} \text{ Nm}^2 \text{ kg}^{-2}$
Mega parsec	$\text{Mpc} = 3.08568025 \times 10^{24} \text{ cm}$
Planck luminosity	$L_0 = 10^{59} \text{ egr/s}$
Mass of the Sun	$M_{\odot} = 1.99 \times 10^{33} \text{ g}$
Kilo parsec	$\text{kpc} = 3.08568025 \times 10^{21} \text{ cm}$
luminosity of the Sun	$L_{\odot} = 3.839 \times 10^{33} \text{ erg/s}$
Positive Cosmological constant	$\Lambda = (10^{16} \text{ ly})^{-2}$
Hubble's constant	$H_0 = 70.65 \text{ km/s/Mpc}$

Symbols

f_{GW}	Gravitational Wave frequency in Hz
L	Total radiated luminosity in erg/s
τ	Time remaining before coalescence in second(s)
M_c	Chirp mass in M_\odot
ρ_{crit}	Critical energy density in eV/cm^3
D_l	Luminosity distance of the from the source to Earth in Mpc
S_{GW}	Power spectral density in unit of egr/sHz

Abstract

Physics of gamma-ray bursts.

1.1 Introduction

what are gamma-ray bursts?

Gamma Ray Bursts (GRBs) are Sudden ,intense , bright and non-repeative flashes of gamma-ray photons of energy in the gamma -ray band (keV - GeV) lasting from a few tens of milliseconds to several minutes.They are the fastest extended objects of Nature, that injecting large amount of energy of order 10^{55} ergs or 10^{47} joules from very small compact region in a few seconds at cosmological distance.The energy released for a few second to hundred seconds comparable to the energy that the Sun will emit in its entire 10 billion years of life time. Furthermore,the overall observed fluence ranges from 10^{-4} ergs/ cm^2 to 10^{-7} ergs/ cm^2 (shown in fig 1.2 , section 1.2), that corresponds to the isotropic equivalent luminosity of 10^{48} to 10^{54} erg s^{-1} [1].

Gamma Ray Bursts (GRBs) are at the intersection of many different areas of astrophysics: they are relativistic events connected with the end stages of massive stars; they reveal properties of their surrounding medium and of their host galaxies; they emit radiation from gamma-rays to radio wavelengths, as well as possibly non-electromagnetic signals, such as neutrinos, cosmic rays and gravitational waves. Due to their enormous luminosities, they can be detected even if they occur at vast distances, and are therefore also of great interest for cosmology [2].

During explosions, ultra relativistic jets are produced accompanied by an intense gamma-ray flashes called prompt emissions that outshine all the sky at very high red shifts.These prompt emissions are often followed by afterglow signals across the electromagnetic spectrum from X-ray to radio wavelengths covering timescales from tenth of seconds up to several months or more [1, 2].

GRB events are classified as being either long (lasting > 2) or short (lasting < 2 s), separated by the length of durations $T_{90} \sim 2\text{sec}$, and spectral hardness of their prompt emissions, with long GRBs (LGRBs) believed to be associated with the deaths of collapsed massive stars, whilst short GRBs (SGRBs) more likely to be the result of either the merger of binary neutron stars (BNS) or the merger of a neutron star with a black hole (NS-BH) [3].

Due to their huge radiated energies, GRBs can be observed up to $z \sim 10$, therefore they are very powerful cosmological tools, complementary to other probes such as SN-Ia, clusters etc. The correlation between spectral peak photon energy $E_{p,i}$ and intensity (E_{iso} , L_{iso} , $L_{p,iso}$) is one of the most robust and intriguing properties of GRBs and a promising tool for measuring cosmological parameters [2, 3].

1.2 Historical Discovery of gamma-Ray bursts

Gamma-ray bursts (GRBs) were first discovered unexpectedly during the Cold War in the late of 1960s by the Vela military satellites that were equipped with detectors of gamma-rays, X-rays and neutrons and launched by USA Air Force in collaboration with the Los Alamos National Laboratory. The first event was recorded in 1967. After verification, it was clear that gamma radiation was not of human origin, nor even terrestrial. However, the existence of Gamma-ray flashes coming from cosmos was announced the first event after six years in 1973 dating back to July 2, 1967 [4].

The study of GRBs physics mainly led by observations with help of improved detecting instruments on satellites to monitor phenomena in the universe in relation to Gamma-ray emissions. Prompted by the instrumental progress from time to time, the story of observational research of GRBs from early time to recent classified in five eras [4] [5].

1.2.1 Dark era (1967-1990)

The first gamma-ray burst discovered named as "GRB 670702" that detected by Vela satellite (see Fig 1.1). In the name "GRB 670702", the first two digits represent the burst year, the middle two and the last two digits represent month and the last

two digits date of the burst. If more than two events of bursts were happened in one day, they labeled to identify them using English letters alphabetically. [4] [5].

After the first discovery , the series of vela satellites were launched ,and more

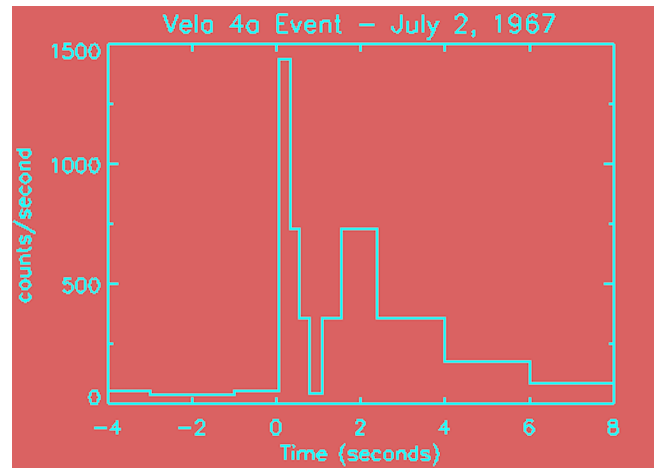


Figure 1.1: Light curve of the first GRB ever detected by Vela. Two separate pulses can be identified over a duration of less than 10 seconds [4]

than 70 GRBs were detected. These earliest observational result of GRBs only consists several structures “spikes” were found in Gamma-ray band ,but no way to identify their location. However,after series of vela satellites were launched with improved detecting instruments ,the origins of GRBs belived to be out side the solar system by offset information [4] [5].

The fundamental questions of the era were : Where are GRBs come from ? What is the source of such flashes of light? By what mechanisms ? do they appear in our galaxy, the Milky Way, or in more distant galaxies ? To answer such questions More than one hundred models were proposed to explain the origin and production mechanisms of GRBs. However, only a few of them were explaining that GRBs events occur at cosmological (at far distances). On the other hand, the majority of the models were indicating that the events of GRBs closer to the Earth (galactic origin) apparently to overcome the energy out put. During the era, the detection and interpretation of GRBs were not progressive due to lack of improved detecting instruments ,however GRBs as new field of science was opened at the end of the era[4][6].

1.2.2 BATSE era (1991-2000)

The Burst And Transient Source Experiment (BATSE) was the early advanced space detecting instruments that carried on the Compton Gamma-Ray Observatory (CGRO), that capable to map Gamma-ray sources from almost the entire sky in energy range of (20keV - 2MeV).The contributions of BATSE in its nine years successful operations were:

- At its early operation in 1991,the apparent isotropic spatial distributions of 2704 GRBs were confirmed (see fig 1.2),and then the cosmological origin of GRBs was accepted by astronomers although the debate between galactic and cosmological origin continued until BeppoSAX. [5][7].

The fig shows,the distribution is « isotropic »: the bursts are distributed randomly on the map indicating that they are either very close to the Earth, or very far, of extragalactic origin. No concentration of bursts along the plane of the Milky Way, symbolized on the map by the horizontal center line, appears. This most likely excludes candidates from our galaxy.

- Fireball model as the theoritical tool to explain the huge amount of energy driven

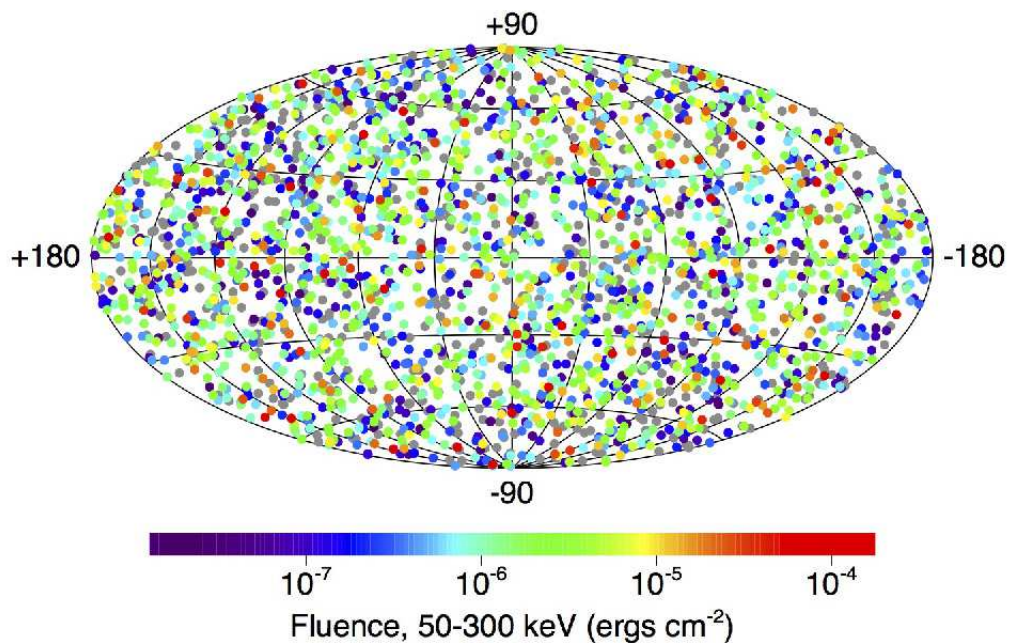


Figure 1.2: The distribution of all 2704 GRBs detected by BATSE satellite: they are clearly isotropically distributed [7].

from observed flux and fast time variability.

- confirm the classification GRBs into two types (short and long GRBs) according to bimodal distribution of durations parameter T_{90} .
- provide database of GRBs, their spectral and temporal properties [5][7].

limitations of BATSE

- unable to classify diversities (single spikey pulses, smooth with or multiple peaks, very erratic, chaotic and spikey).
- BATSE's observations remain limited to gamma-rays alone, no follow-up observations at other longer wavelengths [5][6] [7].

1.2.3 Beppo-sax era (1997-2000)

Beppo-sax equipped with improved instruments on satellite launched in 1997. It was designed to detect long -living afterglows from X-ray to radio wavelength. The contributions of BATSE in its seven years operations were:

- confirm the precise location of the burst in the X-rays rapidly transmitted and also discovered weak and decreasing signals. This was the late-time, weaker emission radiates in the X-rays, optical and radio waves.
- Opened a new era for the current understanding of the mystery of GRBs.
- predicted the existence of GRBs afterglow in longer energy bands (from optical to radio wave length).
- Provide clues for GRB-SN possible connection , which was latter confirmed by HETE-2 and Swift that support collapsar model and explosions of massive star of wolf-Rayet (WR), leaving behind BH.
- Provide crucial informations on the progenitors of GRBs.
- X-ray flash as new class of GRB with less-luminescent and low redshift identified from traditional GRBs [4] [7].

limitation of Beppo-sax

- unable to show the canonical behavior of x-ray afterglow which was later shown by swift [5].

1.2.4 Swift era(2004-now)

The Swift was a robotic spacecraft. It was launched into orbit on November 20, 2004 and orbits at 567 km x 585 km with a period of 95.9 min. is to investigate four phenomena : GRB progenitors, different physical processes underlying different GRB class observations, the interaction between the blastwave and its surroundings, and the early Universe through GRBs. Swift also aimed to investigate other non-GRB-related phenomena. It was the first multi wavelength mission for the study of GRBs, being elaborated by an international collaboration. In its ten years operations, Swift detected more than 2300 GRBs [4] [6].

Swift designed to detect and study the two phases of GRBs : prompt and afterglow emissions, and equipped with three sophisticated detecting instruments working together to observe GRBs and their afterglows in the gamma-ray, X-ray, ultraviolet and Optical wavebands. (see fig 1.3) The instruments and their functions described below: [8][9].

Burst Alert Telescope (BAT).

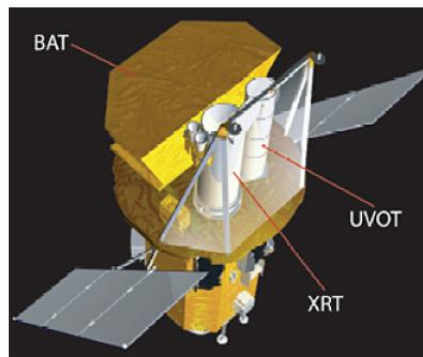


Figure 1.3: Schematic view of the swift satellite (Gehrels et.al 2004). The size of Mask of BAT is $2.7m^2$ [7]

BAT detects GRB event and computes its coordinate (position) in the sky and locates the position of each event with an accuracy of 1 - 4 arcminutes within 15 seconds. This position is immediately relayed to the ground and rapid slew-ground based telescope catches the information.

X-Ray Telescope (XRT)

It takes image and performs spectral analysis of the GRB afterglow. This provides more precise position of GRB with a typical error circle of approximately 2 arcseconds.

radius. The XRT also used to perform long term monitoring of GRB afterglow light curves and operated in energy range of 0.2 keV - 10 keV .

Ultra Violet optical Telescope (UVOT)

UVOT used to detect optical afterglow and provide a sub-arcseconds position. It also used to provide longer wave length follow ups of GRB afterglow light curves. Swift has been a great success in its observations. results include:

- Revealed unusual yet “canonical” X-ray afterglow behavior of X-ray flaring activity during the afterglow phase.
- show the transition from prompt to afterglow emission.

Finally, it detected the high-z GRBs such as 050904,080913 and 090423, which were the most distant cosmic explosions [5] [7].

1.2.5 Fermi era (2008-now)

Fermi designed to focus on prompt emissions phase of GRBs by using much higher energy ranges (8keV - 300keV) than swift (15keV -150keV).It carries on board two types of detectors known to be Gamma-Ray Burst Monitor (GRBM) and Large Area Telescope (LAT).They provide unprecedented spectral coverage for seven orders of magnitudes of energy from 8 keV to 300 GeV.Fermi made Significant progresses for the current understanding of origin of GRBs.

The contributions of Fermi since launched were:

- The existence of three elemental spectral components (Band function-like, thermal and extra non-thermal power-law components) in GRB spectra was confirmed.
- Suggest that the featureless Band function spectra extended from keV to GeV band a Poynting-flux-dominated flow.
- Explain the existence of thermal components in some GRBs(e.g GRB 5090902B) due to hot fireball without strong magnetization.
- The delayed onset of GeV emission in some LAT GRBs suggests that there likely be a change of either particle acceleration condition or the opacity of the fireball during the early prompt emission epoch.
- confirms that long lived GeV emission is likely of external origin, while GeV emission during the prompt phase, on the other hand is likely of internal origin [10] [11].

1.3 Classification of gamma-ray bursts

Based on the bimodal distributions of durations T_{90} or T_{50} of prompt phase or hardness ratio, GRBs have been categorized into two groups: short/hard and long/soft GRBs. The duration of GRB, T_{90} or T_{50} , is defined by the time interval over which 90 % or 50 % of the burst fluence is detected respectively. The typical duration of a GRBs is $\sim 20 - 30$ seconds for long bursts and $\sim 0.2 - 1.3$ seconds for short bursts. Observationally the durations of GRBs can be in a range of 5 orders of magnitude, i.e, from $\sim 10^{-2}$ s to $\sim 10^3$ s. The bimodal distribution of T_{90} has been used to identify the two categories of GRBs, namely, “long” or “soft” ($T_{90} \geq 2$ s) and “short” or “hard” ($T_{90} \leq 2$ s) (see Fig1.4). Instrumentally, T_{90} or T_{50} depends on the energy band and the sensitivity limit of the detector. Theoretically, there are

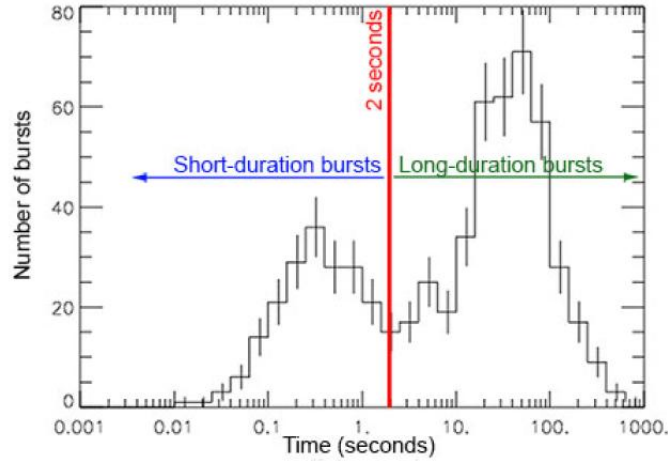


Figure 1.4: The GRB classification (long and short) distribution.

three timescales which may be related to the observed GRB duration T_{90} :

- (1) central engine activity time scale t_{eng}
- (2) relativistic jet launching time scale t_{jet}
- (3) energy dissipation time scale t_{dis} . Then, the observed GRBs duration T_{90} should satisfy: [5]

$$T_{90} \leq \delta t_{dis} \leq \delta t_{jet} \leq \delta t_{eng} \quad (1.1)$$

1.3.1 short/hard gamma-ray bursts

Short/Hard gamma ray bursts (SGRBs) are events with a duration T_{90} less than 2 seconds and account for about 30% of the total gamma ray bursts. They are highly energetic /hard gamma-rays when compared with their long burst counterparts. For

many years short-hard GRBs were not deeply researched as long GRBs. As a result, study of short-hard GRBs (SHBs) is limited. However, one year after Swift launch, in 2005 a breakthrough occurred following the first detections of SHB afterglows [5][6].

The Swift observations established that SHBs are cosmological relativistic sources that, unlike long GRBs, do not originate from the collapse of massive stars, and therefore constitute a distinct physical phenomenon. One viable model for SHB origin is the coalescence of compact binary systems, in which case SHBs are the electromagnetic counterparts of strong gravitational-wave sources. In this burst, the conversion of energy into gamma-rays decreases as the burst progresses. There is no radio, optical, or x-ray counterpart has found for any short burst [5].

1.3.2 long/soft gamma-ray bursts

Another subclass of GRBs that account for 70% and have a duration of greater than 2 seconds are classified as long/soft GRBs (see fig 1.4 above). All long bursts display x-ray afterglow and about one-half as radio or optical afterglows. In long duration bursts energy conversion appears to remain constant through burst. Their creation linked to a young galaxies with rapid star formation and to a core collapse of supernova as well. This is unambiguously associating long GRB with the death of massive stars. Observations of LGRB afterglow at high red shift, are also consistent with the GRB having originated in star-forming regions [6].

1.3.3 Ultra long gamma-ray bursts (ULGRBs)

GRBs with highly a typical durations of more than 10,000sec called ultra-long gamma-ray bursts (ulGRBs). They are the tail end of the standard long GRBs that caused by the collapse of a blue supergiant star, tidal disruption events or a new born magnetar. They have been proposed to form a new third class of GRBs. One explanation which has been proposed for their ultra-long duration is that they could have progenitors differ from classical GRBs in that: they could be produced either by the core collapse of a low-metallicity supergiant blue star, the birth of a magnetar following the collapse of a massive star or the collapse of a Pop III star. In any case, it is clear that the durations of these bursts make them so peculiar that they need further studies [10] [11].

1.4 Global properties of GRBs

Two distinct global properties of “classical GRBs” began to emerge—the intensity /brightness and the angular / location distributions—both are important implications for the distance scale of GRBs and hence their origin.

1.4.1 Intensity distribution

The brightness distribution of GRBs appeared to show that we were seeing out to the edge of the GRB population: there were too few faint GRBs relative to the number expected if GRBs were uniformly (“homogeneously”) distributed in space. Brightness was most straight forwardly measured as the peak flux (P , with units $[\text{erg s}^{-1} \text{ cm}^{-2}]$) in the light curve of a GRB. The brightness distribution is usually measured as the number, $N(>P)$, of GRBs brighter than some peak flux P per year. If the peak luminosity (L , with units $[\text{erg s}^{-1}]$) of all GRBs is the same, then, using the $\frac{1}{r^2}$ law, for a given flux P we would see all the GRBs within a maximum distance: [7] [12].

$$d_{\max} \approx \sqrt{\frac{L}{4\pi P}} \propto P^{-\frac{1}{2}} \quad (1.2)$$

All the GRBs to that distance would be brighter than P by construction. The number of GRBs we would detect to that brightness (or brighter) in one year would just be the volume times the intrinsic rate (R , in units of $[\text{event yr}^{-1} \text{ per volume element}]$): $N(>P) \propto V \times R \propto R \times d_{\max}^3 \propto R \times P^{-\frac{3}{2}}$. So with a homogeneous distribution, we expect that the number of faint GRBs N should grow as a power law proportional to $P^{-\frac{3}{2}}$, where the constant of proportionality scales directly related to the intrinsic rate R : for every ten times fainter in flux we observe, we would nominally expect about thirty-two times more GRBs. While this was indeed seen for the brightest events, there was a flattening at the faint end of the brightness distribution. This flattening was highly suggestive that we were seeing the “edge” of the GRB distribution in space, an important clue in understanding the distance scale. But without knowing the intrinsic luminosity L , we could only infer the shape of the distribution, not the scale. It was like seeing a picture of a building but not knowing if it was of a miniature in a snow globe or the life-sized version [7][12].

1.4.2 Angular distribution

The locations of GRBs on the sky appeared to be randomly (isotropically) distributed: that is, there was no indication that any one direction on the sky was especially more apt to produce GRBs than any other (see fig1.2 in section 1.1). If GRBs were due to neutron stars strewn through out the disk of the Galaxy, for instance, the locations of GRBs on the sky should have been preferentially located near the Galactic plane (as is seen with SGRs). If associated with older stars in the roughly spherical “bulge” of the Milky Way, GRBs would have been preferentially located in the direction toward the Galactic center and less so toward the opposite direction. The inference that the Sun was roughly at the center of the GRB distribution in space, while casting aside some models, still allowed for a variety of distance scales: from a fraction of a light year to billions of light years [7].

1.5 Statement of the problems

As mentioned in section 1.1 above, to study the mystery and phenomenology of Gamma-ray bursts, several satellites (from Vela at early time to Fermi and others at recent time) equipped with different instruments (telescopes) have been launched. Among those satellites, Swift was open new era for the current understanding and development of gamma ray researches. Swift missions detected the prompt and the afterglow emission phases of GRB. Moreover, the temporal and spectral behaviors as well as properties of x-ray and optical light curves of most GRB also studied. However, as far as my search/review literature is concerned, there is a gap knowledge that explaining more about canonical x-ray light curves:

- Does x-ray afterglow the results of internal or external shocks or both?
- What parameters / variables responsible for the variations of temporal and spectral indices of canonical x-ray ;
- what is the implications the variations both indexes.

In this thesis, I emphasized on the theoretical and observational properties of canonical X-ray afterglow light curves qualitatively and quantitatively.

Regarding this work the unclear ideas or un answered questions are listed below. Among these:

- (1) what are the cause of canonical x-ray light curve of afterglow GRB?
- (2) what are the progenitors of canonical x-ray light curves?
- (3) Did the value of temporal index of any random GRB confirmed to the proposed

value in all phases canonical x-ray LCs ?

(4) Could some of the breaks at the end of the plateau phase actually be jet break or late steep decay phase? The goal of this thesis is attempt to explain and give answers for these questions.

1.6 Objectives and thesis outline

General objective

To study how characteristics of light curves gamma ray bursts affected by some parameters or variables such as flux ,luminosity and time.

specific objectives

- To explain the cause and effect for the variations of light curves of prompt and afterglow phases.
- To compare / contrast the proposed values of temporal and spectral indices of x-ray afterglow with/to the calculated values.
- To describe the implications of temporal (α) and spectral (β) indices gamma -ray afterglows.

Thesis outline

Hereafter, I point out the outline of the thesis. In chapter 1 above, the background of gamma -ray physics and a short historical discoveries /explorations/, grb as well as gradual development of them for the past five decades would be discussed. Chapter 2,mainly focused on the production / emission mechanisms of gamma-ray bursts, theoretical and observational properties of grb explained using standard fireball models. Furthermore,the dissipative process(matter- dominated phase) and Radiative process (radiation - dominated phase) of gamma -ray emission mechanisms are explained in detail.

In chapter 3, I address methodology / methods , and models tools used to analyze the temporal and spectral properties of canonical x-ray light curves in swift/XRT for some selected gamma-ray bursts with red shifts two or more breaks. In chapter 4, I discuss on achieved results /findings with proposed values by comparing / contrasting using tables and charts.Finally,I forward a brief summary or review of the enlightenment of this work, as well as a hint for future research in the last chapter.

Emission mechanisms and observational properties of gamma-ray bursts

2.1 Introduction

This section comprises six subsections. Each section contains contents that related to each other in explaining phenomenon of GRBs. Initially, I discussed the emission mechanisms of gamma-ray bursts using different models and processes. In next section, the observational properties of gamma-ray bursts (prompt and afterglow phases), and properties accompanied with them are explained. Thirdly, the early and late time afterglow of GRBs discussed in general. In section four, X-ray as the early afterglow component of GRB would be interpreted deeply. In section five and six, the variation and decaying of luminosity and flux of with time and the calculations presented respectively.

2.2 GRBs production mechanisms

GRB emission /production/ mechanisms:- are the theories or models that visualize or explain how the energy from GRBs progenitor (sources) is turned to radiation. In the early 1990's more than 100 potential models were developed to describe the phenomenon of GRBs. However, more constraining observations over the years have resulted in the development of a 'standard model' to describe the main properties of GRBs with well understood physics.

Over the decades, many theoretical models developed that attempt to explain two main aspects of GRBs: first, what causes the prompt gamma ray and afterglow emission? and secondly, what is the progenitor energy source? For the GRB progenitor, there are two leading models for LGRBs and SGRBs: the core collapse of a massive star and the merger of binary neutron stars (BNSs) or a neutron star

with a black hole (NS-BH), respectively [13].

For further understanding, I reviewed the mechanism that the prompt and afterglow phases of GRBs produced and properties observed during the processes using the theoretical standard fireball model. In general, the fireball model is a neat theoretical model that has been revised in an attempt to explain the mysterious events of GRBs for a longer time.

2.2.1 Basic fireball model

Gamma-Ray Bursts (GRBs) are the most energetic events in the universe. During GRBs impressively high (the most powerful bursts) can eject energy equal to over 9000 supernovae. These energy levels are so extreme that they cannot be created by thermal processes. So, what causes these high energy levels? The Fireball Model is one of the few models that has been put forth to explain why GRBs tend to have such high energy levels. It also attempts to explain the time scales that govern these phenomenon and why they generate an afterglow. More importantly, the model helps to answer pressing questions about GRBs, like why they are so variable (liable to change) over short time scales [13] [14].

Ultimately, it seems that this variability is directly related to the high energy levels, as the variability indicates that it occurs over a very small area with the emission of a GRB being on the order of 10^{52} ergs, coming from a very small region or volume of space with highly concentration of radiation energy, and then theorized that a Lorentz factor of $\Gamma \sim 100$ must be associated with the GRB. In short, the fireball model must be able to encompass all of these variables in order to apply to all GRBs (and thus be a plausible model [14].

The name of the fireball model suggests the mechanism to which a GRB occurs – in a fireball of ultra-relativistic energy consisting of optically thin material with very few baryons. In essence, during the GRB event, the inner engine remains undetectable due to the optical thickness and the lack of a thermal profile due to the compactness of the inner engine. The internal shocks cause the detectable GRB, and the external shocks form the gradual afterglow [15].

The first relativistic fireball model was proposed by (Paczynski 1986, Goodman 1986). They had shown that the sudden release of a large quantity of gamma ray photons into a compact region can lead to an opaque photon–lepton “fireball” through

the production of electron–positron pairs (e^\pm). The most fundamental property the fireball can be characterized by its initial energy E_o . In the fireball there are M_\odot baryons (electrons have negligible mass) with $M_o \ll \frac{E_o}{c^2}$, and its mean energy per baryon, $\eta = \frac{E_o}{M_o c^2}$ [14] [15].

The main prediction of the fireball model is when the expanding plasma becomes optically thin and hence the emitted radiation escapes within the burst formation. As noted above, this mechanism would generate a quasi-thermal spectrum rather than the observed power-law spectra, thus indicating the difficulty inherent to explaining the duration of the GRB having such a small timescale (just a few seconds). Moreover, the fireball baryonic load is another model which converts all its energy into kinetic energy rather than into luminosity to produce a quasi-thermal spectrum. This model, however, does not explain the efficient production of radiation. In particular, the origin of the emission associated with the two phases is produced by two different mechanisms: a matter-dominated, and a radiation-dominated. The assumption that the fireball is matter-dominated is widely used, and which consists of baryons, electrons and positrons, and photons resulting from the merger of binary neutron stars or a collapse of massive stars [10] [15] (see fig 2.1).

The emitted energy is higher than the mass of the baryon in the rest frame by a factor of ~ 100 , with the baryon accelerated with in an expanding fireball to a higher Lorentz factor, Γ . During this process, two major outcomes can be seen: at the photosphere, a fraction of the thermal energy is radiated away and the accelerated electrons produce a non-thermal gamma ray spectrum by a synchrotron or an IC processes in the internal shock at large jet radius. Rather, the outflows that form from the central engine are believed to be dominated by Poynting flux [15][16].

The shocks in the fireball model are collisionless, whereby the particles involved are accelerated and scattered within the Fermi process when crossing the shock interaction. This can result in the type of energy distribution that can be described by a power law ($\alpha \sim 2 - 3$). In such a situation, the electrons emit a non-thermal radiation of photons via two different mechanisms, synchrotron and Inverse Compton scattering, that extend to very high energy (GeV bands). [10] [17].

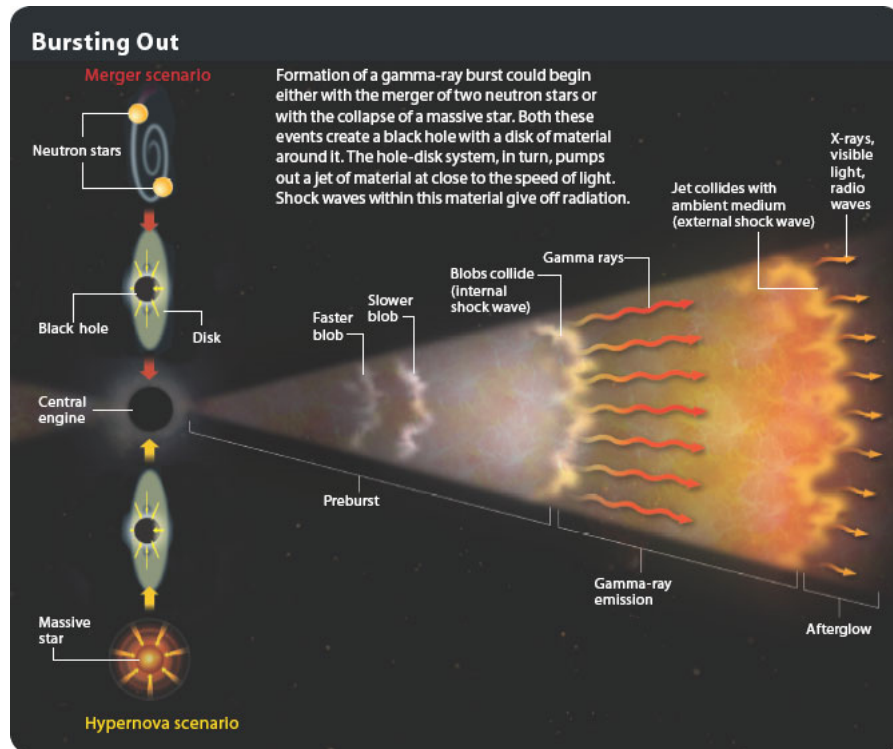


Figure 2.1: Visualisation of the fireball model (from Gehrels et al. (2002), credit Juan Velasco)[13]

Dissipative process

Dissipative process :- is the of outflows or shock waves from central engine interact with interstellar medium (ISM) to produse both GRBs and its afterglow - the external and internal shock models, that successfully interpret the prompt and afterglow emissions respectively. In particular, the origin of the emissions associated with the two phases is produced by two different processes. [8] [17].

Internal shock model

The internal shocks are the mechanism for the production of the observed highly energetic gamma-rays. Moments after the initial GRB event, shock waves emanate from the inner engine at relativistic speeds [99.995% of the speed of light at a Lorentz factor of ~ 100 . The fireball is dynamic; it isn't just one shock wave emanating from the compact source. Instead, different shock waves will be traveling at different relativistic speeds, and it is the interaction between these different shock fronts that cause the energetic gamma-ray emissions [17][18].

The internal shocks traveling at relativistic speeds convert kinetic energy into

gamma-ray photons, this is the only way to get high energy gamma-rays that are observed (as previously mentioned, they cannot be emitted through a thermal process). When internal shocks interact with each other as they are moving at relativistic speeds, the interactions produce Inverse Compton and Synchrotron emissions[18] (see fig2.2).

Initially, the fireball is optically thick but as it expands and cools it becomes

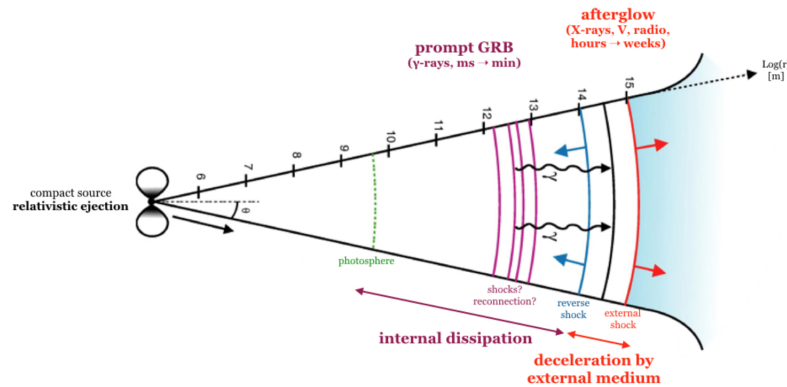


Figure 2.2: Standard fireball model.

optically thin, allowing the gamma-ray photons to escape. Early models had the fireball and the internal shock waves as being purely radiative, but this didn't follow what was being observed (it would have made a profile too smooth). To solve this problem, some baryonic mass was added. This allowed for the internal shocks to become effectively contaminated. The added baryonic mass also aids in the conversion of some radiation energy into kinetic energy, which helps with an added kick to the relativistic kinetic energy of the shock waves, this in turn increases the gamma-ray energy more. Even if all of the shock waves emanate from the core at the same speed they will eventually cross over multiple times. As the shells are emitting through inverse Compton, it is slowing the shock front, thus increasing the times that many shock waves interact with one another. The earlier shock waves are likely to be emitted slower than the later emitted shock waves, this would also increase the amount of interactivity between the different shock waves.[10][18].

External shock model

The external shock waves are used to explain the afterglow that was first detected by BeppoSAX in 1997, as the internal shock waves are not able to explain the

duration of the afterglow nor the wavelengths that are detected (which range from soft x-ray through to radio). The name can be a little misleading at first; the external waves actually refer to the internal waves at a later stage –once they’ve cooled down and continue emanating from the source. As the shock waves continue out they will eventually interact with the Interstellar Medium [ISM] (such as a molecular cloud or some other impedance), and it is the shock waves’ interaction with the dust/gas that cause the afterglow. Unlike the internal shocks, the external shocks are primarily a thermal emission(see fig 2.3). The energy transferred from the shock waves is deposited into the ISM; this material can then be caught up in the shock front and emit radiation. As the shock waves began with a lot of energy, there is a lot that can be deposited into the ISM, this is what can cause such long afterglow and why it covers all parts of the energy spectrum [19].

A relativistic materials/jets are running into some external ambient medium i.e

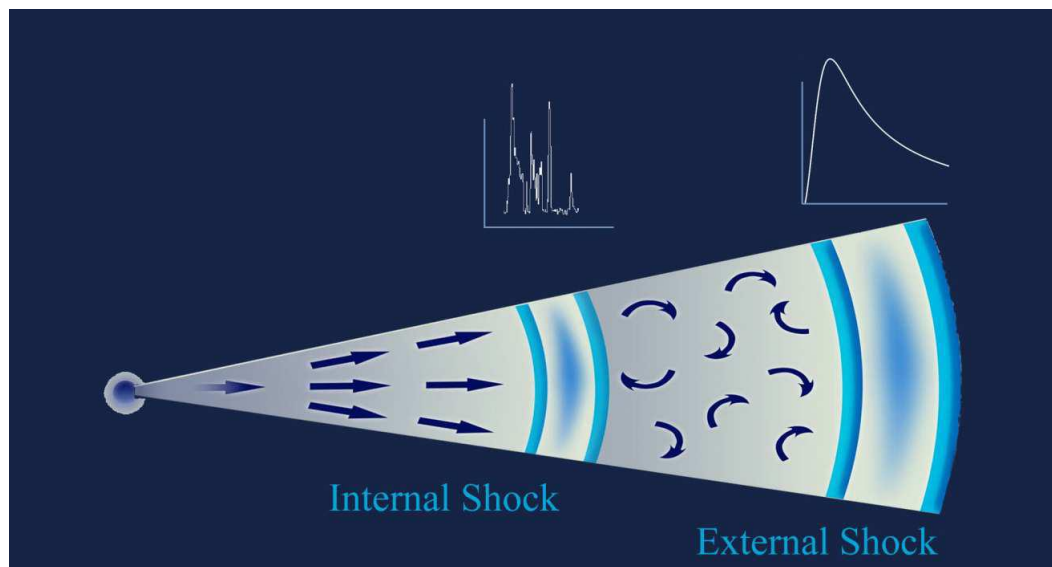


Figure 2.3: Qualitative schematic view of the structure of the relativistic jet produced by the gamma-ray burst. The external shock arises as a result of the impact of the jet on the stellar wind of the progenitor. This is where the final goodbye of the SOS similar emission from the collapsing star forms, which is characterized by a smooth (but non-monotonic) light variation. The internal shock persists as long as the central engine continues operating this is where rapidly varying gamma-, x-ray, and optical radiation forms.

in- terstellar medium or stellar wind. In each time, the ejecta run a high density envi- ronment in which they produced a peak in the mission called external shock [38]. In the external shocks, the jets may be forward shocked or reverse shocked.As

the material in the jet expands, accelerates and compresses interstellar medium, It creates a forward shocks. The deceleration of forward shocks is occurred when the rest mass energy of the swept up particles equal to the ejected energy. This sets a deceleration length scale at ($\sim 10^{16}$ cm) . The reverse shock is formed by the deceleration of the jet material and propagates back into the relativistic flow. This happens when the rest mass energy of the swept up particles is greater than the ejected energy [20].

Although it would be correct to assume that all GRBs have an external shock, about half of detected GRBs don't have a detectable afterglow. The reason that no afterglow is being detected is not thought to be because the exposures aren't long enough, or because we're observing too early or too late. Rather, GRBs occur in high mass systems, whether it be through a supernova or NS-NS and NS-BH merges, this means that they've had very short stellar lives and may still be inside of a molecular cloud. Molecular clouds are very optically thick environments so the reason we're not able to detect the afterglow in about 50% of the time could just be due to reddening, absorption, or scattering.

Radiative process

Synchrotron Radiation

Synchrotron emission is the non-thermal radiation produced when a relativistic electron gyrates in a uniform magnetic field. Synchrotron radiation can explain the GRB prompt emissions, and is considered to be one of the more important mechanisms in various astrophysical phenomena. The synchrotron shock mechanism, which is produced by the optically thin plasma in a weak magnetic field, can be used to predict the form of the observed spectra [1][15][18]

Synchrotron emission can be classified as having two regimes: the "fast-cooling" phase, which describes when the timescale for the cooling of the electrons is shorter than the dynamical lifetime of the source, resulting in an electron that cools quickly compared to the low-level injection of energy; conversely, "slow-cooling" occurs when the timescale for the cooling of the electrons is longer than the dynamical lifetime of the source . The differences between these two regimes are associated with the emission's radiative timescale [9] [10].

The peak frequency, the cooling frequency, and the self-absorption frequencies set

the characteristic break frequencies in the synchrotron spectra. These frequencies evolve with time; indeed, their evolution is reflected in the complexities observed in the shapes of the light curves at certain band energies. This model can successfully describe the afterglow. Thus, the optically thin synchrotron spectrum is currently considered the best spectral fitting model for most GRBs. The first synchrotron model was applied to the spectral fitting of GRBs by Tavani (1996), and subsequently by Baring and Braby (2004) [15][16].

Synchrotron Self-Compton

Inelastic collisions between low-energy photons and ultra-relativistic electrons are known as the IC processes. Each astrophysical source has an Synchrotron Self-Compton (SSC) scattering component when synchrotron radiation that energizes it provides the means to scatter its seed photons to high energies and across a large frequency range. Thus, the phenomenon responsible for creating high-energy emissions from GRBs and other astrophysical sources is accepted to be the SSC mechanism. The SSC mechanism, while complex, uses a simple power-law function to explain the injected electron spectrum. The SSC spectrum can be described precisely as carrying out a complicated seed photon spectrum convolution and electron energy distribution. In certain circumstances, the GRB spectrum can be modelled as an SSC component at very high energy ~ 10 MeV. [11][16]

2.2.2 progenitors of GRBs

2.2.3 Working mechanisms of central engine

The inner engine is of great importance, as it needs to be able to push material out very near the speed of light. The inner engine of a GRB is a highly compact source, and it is the highly compact nature of this object that leads to the idea that the core of the inner engine of a GRB is either a neutron star or a black hole (as they're the two most compact sources that we're currently aware of) The workings of this inner engine will alter depending on whether it is a long or short GRB being observed. A short GRB has been theorised as occurring during a neutron star binary collision [NS-NS] or a neutron star-black hole collision [NS-BH]. It has been suggested that a long GRB could be associated with a hypernova – a Wolf-Rayet type star undergoing a core collapse supernova. [21]

2.2.4 GRB-SN association

2.3 GRBs Observations and interpretations

GRBs composed of two main radiative phases: the prompt and afterglow phases. The former typically observed in soft gamma-ray (10 keV to 10 MeV), and generally lasts between $\sim 100\text{ms}$ and $\sim 1000\text{ s}$, although there is a wide variety of different temporal behaviors observed, from single pulses to complex temporal evolution. The spectrum of this prompt emission is non-thermal, often described by a Band function with a typical peak around $\sim 200\text{ keV}$. The afterglow emission is most often detected from X-rays to radio waves and fades with time. In the optical, the temporal fading goes typically as t^{-1} , however the slope of this fading depends on the wavelength and on the burst. This means an afterglow observed in the optical will frequently fade beyond the reach of most ground-based telescopes within a week. In the radio however, there is evidence of emission from the afterglow up to a few months or even years after the burst. The sudden flash of gamma rays emitted in the creation of a GRB was the route by which GRBs were detected and the property for which they are named. The prompt emission is readily detected, even by rudimentary space-based gamma-ray detectors, due to the extreme high-energy photon budget that GRBs exhibit. Indeed, at peak, GRBs outshine all other sources within gamma-ray sky, including the Sun.[18]

2.3.1 prompt GRB emission

prompt emission of GRBs is defined as the emission observed during the gamma-/hard X-rays phase, whose photons are the ones triggering the space instrumentation leading to multi-wavelength follow-up observations. It is believed to be the direct outflow ejected from the central engine; as per the "fireball" model, which deposits its gravitational energy into a thermal explosion. In other words, the prompt emission occurs when the kinetic energy from a catastrophic explosion event, such as massive star core collapse or the merger of two compact stars, is converted into electromagnetic radiation due to the internal shocks that result from collisions between shells of ejecta.[23]

prompt emission generated due to internal shocks magnetic dissipation within

the fireball take place effectively above the pair production photosphere at 10^{12} to 10^{14} cm. These shocks split from mini-shells within a jet produced by unsteady accretion of materials onto black hole or by the merger of binary neutron stars (BNS). The shells have a distribution in lorentz factor $\gamma \propto \Gamma$ where Γ is bulk lorentz factor.[22][23]

In the region around $\sim 10^{12}$ cm to 10^{14} cm , the collisions between different parts of

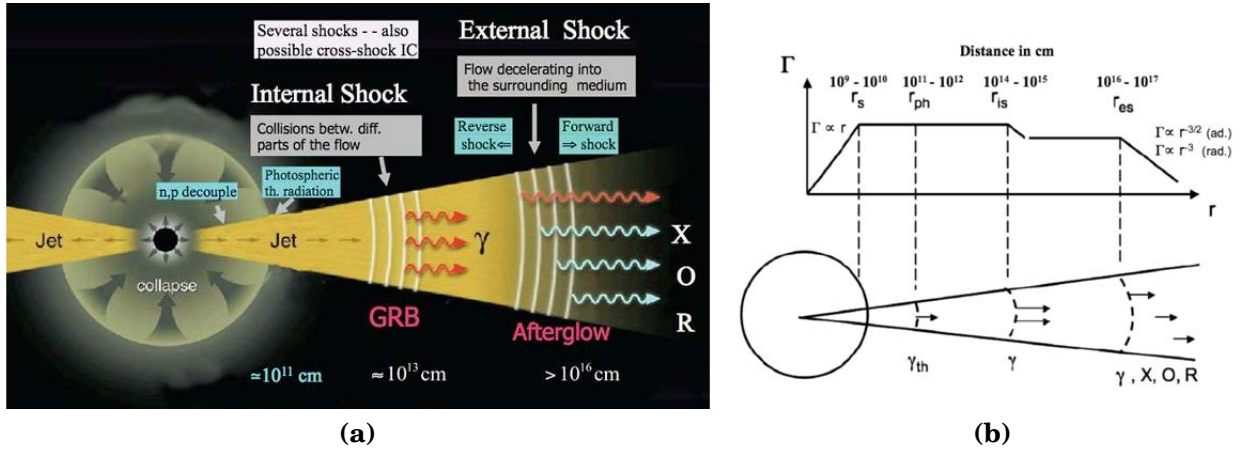


Figure 2.4: Schematic evolution of the jet Lorentz factor and examples of symbolic locations of radius: the saturation radius r_s , photospheric radius r_{ph} , internal shock radius r_{is} and external shock r_{es}

the flow is produced in different shells (see fig 2.4 (a) and(b)). As a fast shell catch up with a slower ones, they form strong internal shocks that propagates in both shells with out deceleration. Once shell became above the photosphere, the heated and accelerated electrons cool by synchrotron emission then radiation is observed in γ -ray band. Each collision that occurs above pair photosphere produces a pulse in the GRB's light curves[22]

Thus, GRB light curves represent the count rates/photons recorded by the high energy detectors as a function of time. Each of the recorded events shows different variability patterns, meaning that each light curve is different from the rest. As it is shown in Figure 2.6, the light curves can be classified into four different categories Pe'er, 2015:

- single-peak events (e.g. GRB 910711),
- a smoothed light curve composed with several peaks (e.g. GRB 920221),
- separated multi-collisions (e.g. GRB 930131A),
- and irregular peaks (e.g. GRB 991216)

The result is that the fireball expands due to the effects of thermal pressure and

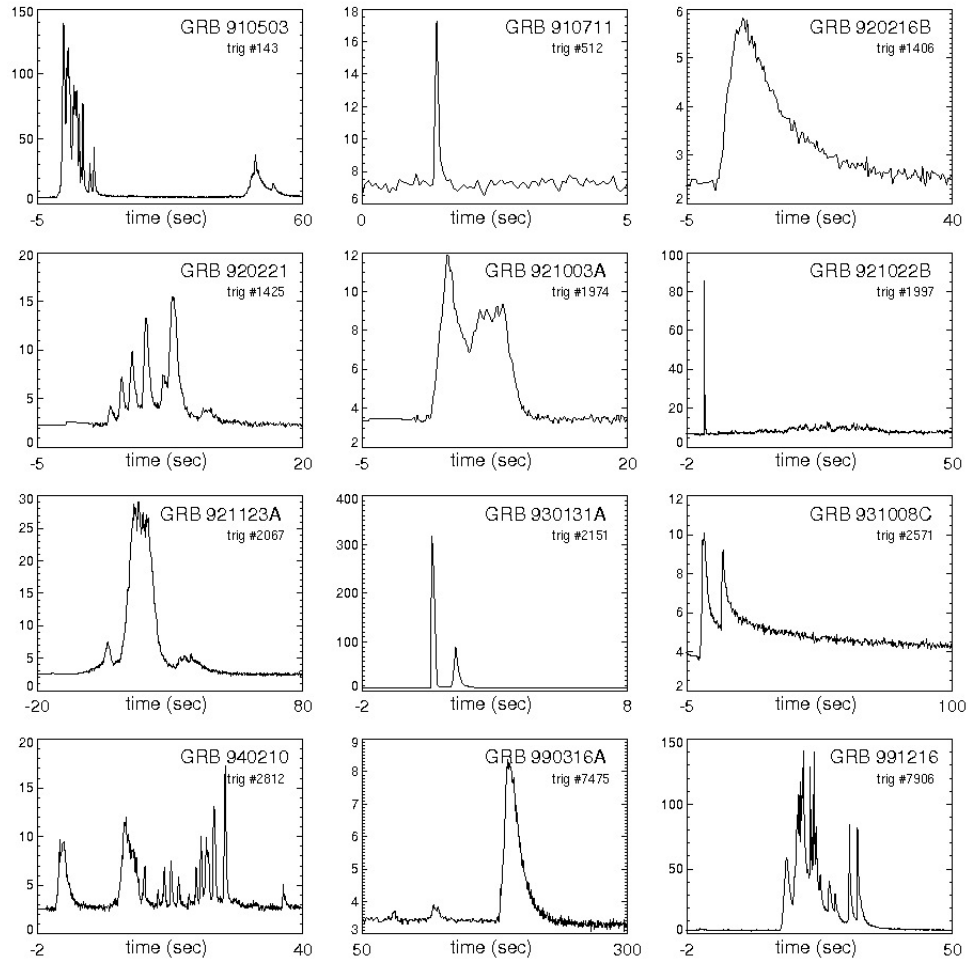


Figure 2.5: Diverse light curves of the GRBs prompt emission detected by BATSE instrument. This sample includes short and long events. <https://gammaray.nsstc.nasa.gov/batse/grb/lightcurve/>

[Firaol Fana]

is then accelerated to relativistic speeds, where the thermal energy is ultimately released in the form of photons at the photosphere. In the internal shock case, the dissipation happens inside the ejecta, where the ejecta is decelerated by the surrounding medium and this deceleration happens after the internal shock phase ceased. [6][10][23]

2.3.2 Afterglow GRB emission

Afterglow is the phase of GRBs that slowly fading at longer wavelength. This emission is created by the collision between ejected bursts and the surrounding medium or interstellar gas or dust. The GRB itself is rapid, lasting from less than a second up to a few minute at most. Once it disappears, it leaves behind

a counterpart at a longer wavelengths from X-ray to radio bands . Then, they are remain detectable for day or longer. As we have mentioned above, afterglow emissions are dominated by external shocks. Due to lack of advanced instrument, early searches were unsuccessful largely to observe the bursts' position at a longer wavelength immediately after the initial burst. Once the GRB faded deep imaging was able to identify a faint, distant host of galaxy at a location of GRB as pinpointed by the optical afterglow.[15][22][23]

2.4 Interpretations of GRBs afterglow

Before launch of the Swift satellite, broad-band, late time ($t > \sim 10$ hours) afterglow data had been collected for a moderate sample of GRBs. These observations were generally consistent with predictions of the external forward shock, synchrotron emission, model. The main observational properties of late time afterglow radiations are:

- In general the optical afterglow displays a power law decay behavior $F_\nu \propto t^{-\alpha}$, with a decay index $\alpha \sim 1$. This is consistent with the prediction of the standard external shock afterglow model.
- A temporal break in the optical afterglow light curve is usually detected for bright GRBs. The break time is typically around a day or so, which is followed by a steeper decay with slope $\alpha \sim 2$. This is consistent with the theoretical prediction of a “jet break”.
- The radio afterglow light curve initially rises and reaches a peak around 10 days, after which it starts to decline (e.g. Frail et al., 2000). The peak usually corresponds to passage of the synchrotron injection frequency ν_m , or the synchrotron self-absorption frequency ν_a , through the radio band.
- The broad-band afterglow spectrum can be fit with a broken power law, at a fixed observer time as one expects for the synchrotron afterglow model.
- For bursts with high-quality data richer features in the optical light curves have been discovered, which include bumps and wiggles that deviate from the simple afterglow model predictions. Smooth bumps in afterglow lightcurves with duration $\delta t_{obs} \sim t_{obs}$ may be interpreted as due to density bumps in the external medium where as sharper features in lightcurves might be due to energy injection from the central engine angular fluctuations in energy per unit solid angle [18].

2.4.1 Early time afterglow

2.4.2 Late time afterglow

Before swift mission, afterglow observations was started after several hours (and 10 hrs) after bursts trigger. The optical afterglow of late time afterglow displays a power law decay behavior $F_\nu \propto t^{-\alpha}$, with a decay index $\alpha \sim 1$. The temporal break in the optical afterglow light curve was detected for bright GRBs. The break time is typically around a day and followed by the steeper decay with decay slope of $\alpha \sim 2$ [24]

The radio afterglow light curve initially rises and reaches a peak around 10 days after which starts to decline. The peak usually corresponds to the passage of synchrotron injection frequency ν_m or synchrotron self absorption frequency ν_a through the radio band. The broad band afterglow spectrum can be fit with a broken power law at a fixed observer time.[25]

2.5 Theoretical interpretation of X-ray afterglow

Afterglow GRBs observed at all wavelengths such as: X-ray [26], optical [27], IR, and radio [28]. Thanks to its low variability and observed time range (from minutes to weeks after the GRB event), a canonical X-ray light-curve for the afterglow was defined from the result of Swift /BAT-XRT instruments. (It is displayed on Fig2.6). From the fig, the 0 symbol indicates the prompt phase, and the four remaining segments, with their corresponding temporal indexes, are associated two by two and identified as early and late afterglow [29],[30][31]: I and II (respectively the steep and shallow decay), and III and IV (respectively a standard afterglow and a jet break). Part I and III, marked by solid lines, are most common and the other three components, marked by dashed lines, are only observed in a fraction of all bursts. Part I, thought to be associated with the prompt phase when the central engine is still active; the rest of the afterglows are due to the dynamics of the interaction between the jet and the surrounding medium.[6][15][18] [32].

The detection of GRBs early afterglows is within less than 100 seconds after trigger in the swift mission. The canonical X-ray afterglow light curve generally includes four phases such as early time steep decay phase, the shallow decay /plateau phase, normal decay phase and late steep decay phase [33].

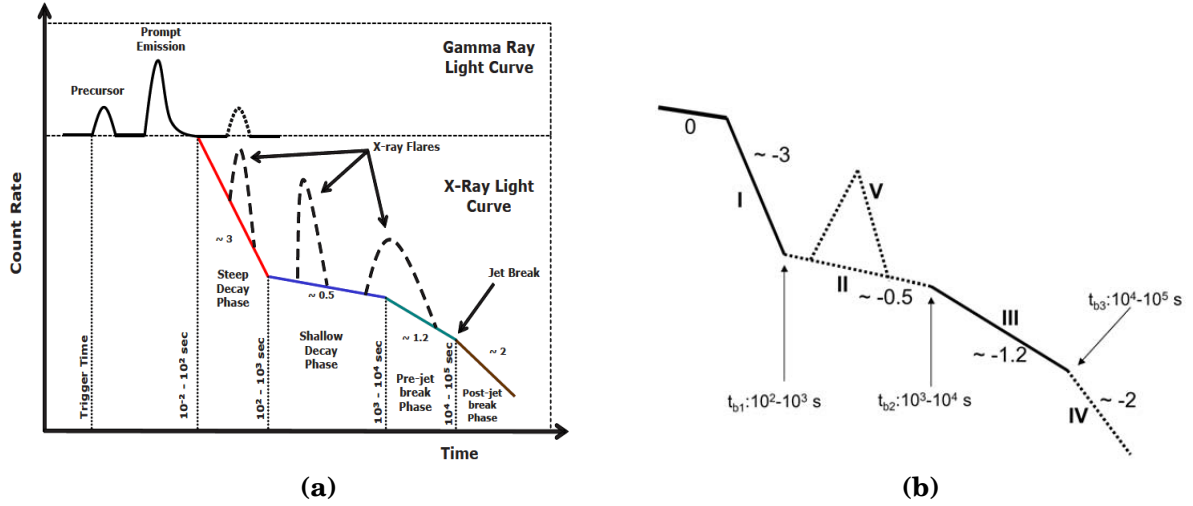


Figure 2.6: Canonical GRB light curve. The prompt phase is often followed by a steep decay phase (typical index of 3) which can then break to a shallower decline (shallow decay phase), a standard afterglow phase (pre-jet break phase), and possibly, a jet break and post-jet break phase. Sometimes an X-ray flare is seen.

2.5.1 steep decay of early X-ray light curves

. This phase is the tail of prompt emission that governed by curvature effect, for which emission from different viewing angles reaches the observer with different delays due to the light propagation effects [33]. The relationship between temporal and spectral slopes of higher latitude emission is $\alpha = 2 + \beta$. It is independent of any of the environmental or other parameters such as peak frequency and cooling frequency that affects the closure relations for the external shocks.

Swift answer the debate of separation between prompt emission and late afterglow regarding to internal and external origin of the prompt emission i.e internal shocks are the origin of prompt emission [33]. As it has shown in (Fig2.6 above), slope of early steep decay is around $3 < \alpha_1 < 5$. This phase may be simply the high latitude emission associated with the prompt gamma-ray sources at $R \gtrsim 10^{15}$ cm when the central engine turns off faster than the decline of the X-ray light curves . On the other hand, if the emission region is at much smaller radius than the rapidly declining X-ray light curve reflects the time dependence of central engine activity[36].

Detailed analysis of a sample of GRBs suggests that the high latitude "curvature effect" model can explain the early steep decay phase [37]. As we have shown in

(Fig 2.5), the achromatic change of phases for sample GRBs indicates the light curves transition. These GRBs followed the decay power law relation $F_\nu \propto t^{-\alpha_1}$ where, $\alpha_1 = 2 + \beta$ for curvature effect model. Generally, this phase has already stayed between the time interval of $10^{-2} - 10^2$ seconds and $10^2 - 10^3$ seconds that presented (in fig 2.6) at the right side.

2.5.2 Shallow /plateau decay X-ray light curves

This phase is sometimes called plateau phase and very small decay with value of decay $0.5 < \alpha_2 < 1.0$. This phase rises when the energy ejected to the decelerated external shock. When the energy is terminated, the decay of light curves become slow down and the transition to phase three (normal decay) is occurred [51]. In this phase, the shape of light curves in the X-ray and optical bands should be similar where break occur at the same time in these bands.[38][39] .

There are two acceptable explanations behind the emission mechanisms of this phase. (1) A smooth and gradual energy injection that arrives in the forward shock, is due to the decrease of the lorentz factor Γ at the end of prompt emission. The mass that is injected to the forward shock is the function of its lorentz factor and the energy injected. As a result Γ increases monotonically with radius,(which we discussed in detail in section (2.6). The flux decays are a power law and depends on the mass and the energy injected . (2) The central engine of the source stays active for hours after the burst and injects the smooth and continues energy at later times, several times after the burst[40] [41].

X-ray plateaus results from the contribution of prompt X-ray emission scattered by dust in the host galaxy. The optical flux or the powerful outburst episode is already ruled out by the prompt optical data[42].

2.5.3 normal decay phase

This is the third phase in this canonical phase description. This phase has a decay slope around $1.0 < \alpha_3 < 1.5$ which was expected before swift and it is consistent standard fireball afterglow model in ISM [56]. The explanation of this phase is related to the end of energy injection at the external shocks. This implies (1) the fall of the lorentz factor of forward shock up to the point of minimal lorentz factor that carries a significant initial energy. (2) The time that the central engine needs

to be in active. In general the normal decay is expected in the standard forward shock.[43]

2.5.4 Late steep decay following the plateau in X-ray light curves

The early steep decay represented at the left side of fig 2.6 , the decay slope is greater than 2. After the normal decay, X-ray emission is powered by a continues jet from a long lasting central engine. Then X-ray flux from the external shock is buried beneath this emission [58]. Indeed, the canonical X-ray light curve can be matched with the accretion history in the collapsar GRB model. This model assume that the X-ray luminosity is proportional to the accretion power of the central engine [59]. This late steep decay of swift, represents an achromatic steepening that happens due to the jet breaks. When the lorentz factor of the ejecta becomes larger than θ_0^{-1} compared to the jet opening angle θ_0 , the ejecta is collimated into a jet break. Finally, this phase is expected in the forward shock model as a jet break. Jet breaks are thought to happen due to the beaming of the emission from GRBs. This phase has pre-jet-break phase and post-jet-break phase, (see in Fig 2.6).[44] [?]

2.5.5 Time breaks in swift X-ray afterglow

As shown in (Fig 2.6), there are three break points and the time at that points are called breaking time of afterglow light curves. These break times are the first break time, the second break time and the jet break time.

2.5.6 The first break in the light curve ($t_{break,1}$)

This is the time at which the phase change of light curves from phase I to phase II is took places. As we have shown in (Fig2.6), the $t_{break,1}$ is around $t_{break,1}(10^2 - 10^3)$ s $< t_1 < t_{break,2}(10^3 - 10^4)$ seconds).

The first break time is also the time when the slow decaying emission from the forward shock become dominant over the rapidly decaying flux from the prompt emission at a large angle. In sharply decaying flux, the prompt emission initially dominates over the external shocks at $t > t_{break,1}$ [?].

2.6 Decay of flux with time of observed light curve

The fluence (S) is the total radiant energy collected from the GRBs per unit area over the duration of the event (i.e., T_{90}). It is computed by integrating its energy flux over time and the energy range of the detector (i.e., the total energy collected per unit time and per unit area). The fluence measured between energies E_{min} and E_{max} is given by[Firaol Fana]

$$S = T_{90} \int_{min}^{max} E \frac{dN}{dE} dE \quad (2.1)$$

The energy flux of a burst is defined

$$F = \int_{E_{min}}^{E_{max}} E \frac{dN}{dE} dE \quad (2.2)$$

When relativistic, conical and optically thin source moving with a lorentz factor Γ turns off abruptly, the flux declines rapidly with time [47]. In such type of source which is specified with spherical co-ordinate (r, θ, φ) , the source turned off at $r = R_0$. where r is the radius of the photo/jets, R_0 is the radius of the observer and θ is measured with respect to the line of sight to the observer. The time dependence

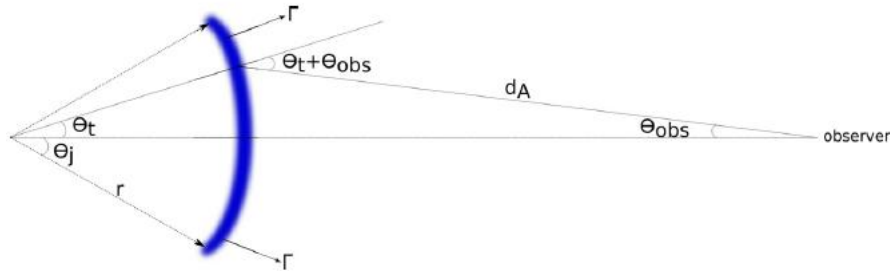


Figure 2.7: A sketch of the various angles and distances for the large angle (or high latitude) emission when the γ -ray source turns off suddenly.

of observed flux follows from the lorentz transformation of specific intensity. The specific flux in the observer frame from the relativistic source of moving object with specific intensity $I_{\nu'}$ and spectrum frequency $\propto \nu'_{-\beta}$ is given by

$$f_{\nu}(t_{obs}) = \int d\Omega_{obs} I_{\nu} \cos \theta_{obs} \quad (2.3)$$

where $d\Omega_{obs}$ is the solid angle of the source, I_{ν} is the specific intensity of the source photon. To derive the standard flux decay of GRBs, let we define $d\Omega_{obs}$ and I_{ν} in the

relativistic beaming.

In relativistic beam of photons, the transverse component of the momentum does not change under lorentz transformation, i.e its comoving and lab frame values are the same. Thus

$$\nu \sin \theta = \nu' \sin \theta' \quad (2.4)$$

or

$$\sin \theta = \frac{\nu'}{\nu} \sin \theta' \quad (2.5)$$

Since the photon frequency on the observer frame, ν , can be expressed in terms of the comoving frequency, ν' , using standard lorentz transformation of photon as

$$\nu = \frac{\nu'}{\Gamma(1 - \frac{v \cos \theta}{c})} = \nu' D \quad (2.6)$$

where D is standard doppler effect which is expressed as $[\Gamma(1 - \frac{v \cos \theta}{c})]^{-1}$. Then the ratio of the frequency become $\frac{\nu'}{\nu} = \frac{1}{D}$ and substituting this ratio into Eq. (2.5), we obtain

$$\sin \theta = \frac{\sin \theta'}{D} \quad (2.7)$$

For large Γ , $\theta \approx \frac{\theta'}{\Gamma}$. This tells us photons are focused in the forward direction such that the angular size of photo beam in the lab frame is smaller than it is in the comoving frame by a factor $\sim \Gamma$. And also the solid angle for a canonical beam of photons in lab frame is smaller than in the comoving frame by a factor of $\sim \Gamma^2$. This implies the lorentz transformation of solid angle is:

$$d\Omega = \sin \theta d\theta d\phi = \frac{\sin \theta' d\theta' d\phi'}{D^2} = \frac{d\Omega'}{D^2} \quad (2.8)$$

The other parameter in the lorentz transformation is the specific intensity. It is defined as flux per unit frequency and solid angle carried by photos traveling with in a narrow conical beam with its axis perpendicular to surface dA . This means

$$I_\nu = \frac{dE}{d\nu dt_{obs} dA d\Omega} \quad (2.9)$$

Considering $d\nu' dt' obs dA' = d\nu dt_{obs} dA$, are lorentz invariants and using Eq. (2.8) and $E = \Gamma E'$, Eq. (2.9) can be reduced to

$$I_\nu = D^3 I'_{\nu'} \quad (2.10)$$

Since for intrinsic spectrum, $I'_{\nu'} = I' \nu'^{-\beta}$, where β is spectral index, then the specific intensity is summarized as

$$I_\nu = D^3 \nu'^{-\beta} I' \quad (2.11)$$

This equation, can be simplify by substituting the value of ν' from the Eq. (2.6)

$$I_\nu = D^{3+\beta} \nu^{-\beta} I' \quad (2.12)$$

Finally substituting Eq. (2.8) and Eq. (2.12) into Eq. (2.3) and integrating over $d\phi$ in the interval $0 - 2\pi$, the observed flux becomes

$$f_\nu(t_{obs}) = 2\pi \int d\theta_{obs} \frac{I'_{\nu'} \nu_0'^\beta \sin 2\theta_{obs} [(1+z)\Gamma]^{-(3+\beta)}}{2\nu^\beta (1 - v \cos(\theta + \theta_{obs})/3)^{3+\beta}} \quad (2.13)$$

where ν'_0 is the frequency that lies on the power law segment of the spectrum for $I'_{\nu'}$. Using the law of sine from the diagram in Fig. 2.7, we see that $\sin\theta/dA = \sin\theta_{obs}/R_0$, this implies $\sin\theta_{obs} = \frac{R_0 \sin\theta}{dA}$ and substituting into Eq. (2.13), in the case $\theta_{obs} \ll \theta$, yields

$$f_\nu(t_{obs}) = \frac{2\pi I'_0 \nu_0'^\beta \nu^{-\beta}}{[(1+z)\Gamma]^{3+\beta}} \left(\frac{R_0}{dA}\right)^2 \int_{\theta_t}^{\pi/2} d\theta \frac{\sin\theta \cos\theta}{(1 - v \cos\theta/c)^{3+\beta}} \quad (2.14)$$

Using substitution method of integrating, this equation can be simplified as

$$f_\nu(t_{obs}) \propto \left[1 - \frac{v \cos\theta_t}{c}\right]^{-(2+\beta)} \nu^{-\beta} \quad (2.15)$$

Photons released at $(r=vt, \theta, \varphi)$ arrive at the observer frame with a time delayed to a photon emitted at $r=0$ of

$$t_{obs} = t - \frac{\theta}{c} = t \left(1 - \frac{v \cos\theta}{c}\right) = t/\Gamma D \quad (2.16)$$

From this equation, the relation between t_{obs} and D is $t_{obs} \propto D^{-1}$. Then the flux decay with time of the observed light curves from Eq. (2.15) is summarized as

$$f_\nu(t_{obs}) \propto t^{-(2+\beta)} \nu^{-\beta} \quad (2.17)$$

The standard convection of flux decay is

$$f_\nu(t_{obs}) \propto t^{-\alpha} \nu^{-\beta} \quad (2.18)$$

where $\alpha = 2 + \beta$

2.7 calculating luminosity (L) of x-ray afterglow

Luminosity is the total amount of electromagnetic energy radiated (out put) by an object per unit of time. The observed isotropic-equivalent luminosity in the X-ray afterglow, L_x can generally be expressed as

$$L_x(t) = \int_{\nu_1}^{\nu_2} L_\nu(t) d\nu \quad (2.19)$$

where $L_\nu(t) = \frac{4\pi d_L^2 F}{(1+z)}$, substituting $L_\nu(t)$ in to equa. (2.4) reveals

$$L_x(t) = \frac{4\pi d_L^2}{(1+z)} \int_{\nu_1}^{\nu_2} \frac{F_\nu}{(1+z)[(1+z)t]} d\nu \quad (2.20)$$

where d_L is the luminosity distance, ν_1 and ν_2 are the spectral frequencies in the energy band, z is the redshift and $L_\nu(t)$ is the spectral luminosity at the cosmological frame of the source, i.e, both ν and t are measured in the frame [62].

$$L_x(t) = 4\pi d_L^2 \int_{\nu_1/(1+z)}^{\nu_2/(1+z)} F_\nu[(1+z)t] d\nu \quad (2.21)$$

since $F(t)$ is measured in the observer frame and assumed in standard form, Eq. (2.21) can be reduced to:

$$L_x(t) = 4\pi d_L^2 (1+z)^{(\beta-\alpha-1)} F_x(t) \quad (2.22)$$

where $F_x(t) = \int_{\nu_1}^{\nu_2} F_\nu(t)$

Here, we have understood that the flux decay of afterglow light curves are governed by standard power law of decay, i.e $f_\nu(t_{obs}) \propto t^{-\alpha} \nu^{-\beta}$, where $\alpha = 2 + \beta$. This is a theoretical understanding for the afterglow era. Therefore, swift observation have led to the better understanding of afterglow x-ray light curves for the initial few hours. The two mechanism of emissions have related to the behavior of central engine of the burst. Now let we introduce the methodology of analyzing the temporal and spectral indices of the afterglow in the next chapter.

Research methodology

Introduction

After the launch of the Swift , observational and theoritical understanding of the prompt and afterglow phases of gamma-ray bursts promptedly changed due to use of satellites equipped with improved detecting instruments. Furthermore,the debating issues at early dicoverly: the sources , the cosmological origin and isotropic distributions of GRBs were confirmed in swift era. Not only these , standared models " fire ball model " developed to explain the emmission mechanisms of gamma-ray burst and its afterglows (from X-ray to radio band).However,to achieve objectives of this study , un explained ideas and knowledge gaps that appeared in review litrature shouldbe answerd.Therefore,appropriate and comperhensive methodology i.e , quantitative and qualitative research approaches and procedures are implemented.

3.1 Research designs

Modeling

As we have mentioned in section (2.2), the standard fireball model proposed to explain afterglow gamma-ray bursts. In standard fireball model, the behavior of X-ray light curves is assumed to be a single power law decay where flux fads as:

$$f_{\nu}(t) \propto t^{-\alpha} \quad (3.1)$$

where f_{ν} the flux decay with time and α is the temporal index/decay slope and subscripted by numbers $\alpha = 1, 2, 3,$ and 4 for early steep decay slope, shallow decay slope, normal decay slope and late decay slope respectively , that were captured by the swift/XRT. This is the model that relates both temporal(α) and spectral(β) indices in standard fireball model as: $\alpha = 2 + \beta$ called the closure relation , where both β and α are unitless.

Simple emperical model

3.2 Data sources,sampling techniques and size

In our synthesis of swift XRT light curves, I have been selected 10 GRBs as a representative sample from which 5 are long GRBs and the other 5 are short GRBs with known red shifts and have one or two light curve breaks for analyzing data. The selection criteria were number of light curve breaks , types of gamma-ray bursts and known redshifts.

3.2.1 Data sources and types.

I use secondary data from Evans et al online repository(swift/xrt) already collected during observations over longer time.

3.2.2 Data sampling technique and size

For our data analysis 10 GRBs are selected using simple random probability sampling method.

3.3 Validity and reliability of data

3.4 Data processing and analyzing

3.5 Evaluating and justifying methodology

Result And Discussion

4.1 Introduction

Conclusion

Bibliography

- [1] Piran, Tsvi The physics of gamma-ray bursts, *Reviews of Modern Physics*,76 (4);1143,2005
- [2] Gomboc, Andreja Unveiling the secrets of gamma ray bursts, *Contemporary Physics*, 53(4):339–355, 2012.
- [3] Gehrels, Neil and Ramirez-Ruiz, E and Fox, Derek B Gamma-ray bursts in the Swift era, *arXiv preprint arXiv:0909.1531*, 2009.
- [4] Turpin, D and Heussaff, V and Dezalay, J-P and Atteia, JL and Klotz, A and Dornic, D Connecting Prompt and Afterglow GRB emission I. Investigating the impact of optical selection effects in the Epi-Eiso plane, *arXiv preprint arXiv:1503.02760*, 2015.
- [5] Zhang, Binbin A Multi-wavelength study on gamma-ray bursts and their afterglows,2011
- [6] Dereli, H Study of a Population of Gamma-ray Bursts with Low-Luminosity Afterglows, submitted to *astroph(-)* ,*arXiv preprint arXiv:1503.04580*,2014
- [7] Hu, You-Dong Multi-wavelength study of GRBs detected by Fermi and Swift,2021
- [8] Margutti, Raffaella and Zaninoni, E and Bernardini, MG and Chincarini, G A comprehensive statistical analysis of Swift X-ray light-curves: the prompt-afterglow connection in Gamma-Ray Bursts, *arXiv preprint arXiv:1207.0537*,2012
- [9] Gupta, Rahul and Oates, SR and Pandey, SB and Castro-Tirado, AJ and Joshi, Jagdish C and Hu, YD and Valeev, AF and Zhang, BB and Zhang, Z and Kumar, Amit and others. GRB 140102A: insight into prompt spectral evolution and early optical afterglow emission, *Monthly Notices of the Royal Astronomical Society*,505 (3);4086–4105,2021

- [10] Moneer, Eman Spectral Analysis of GRBs Observed by Swift and Fermi Satellites;2019
- [11] Massaro, Francesco and Thompson, David J and Ferrara, Elizabeth C The extragalactic gamma-ray sky in the Fermi era, *The Astronomy and Astrophysics Review* ;24(1);1–58,2016
- [12] Sari, Re'em and Piran, Tsvi Variability in GRBs-A Clue;Arxiv preprint astro-ph/9701002, 1997
- [13] Knust, Fabian Applying the Fireball Model to Short Gamma-Ray Burst Afterglows: Methods, Jet Opening Angles and Plateau Phases,2017
- [14] Dainotti, MG and Del Vecchio, Roberta Gamma Ray Burst afterglow and prompt-afterglow relations: An overview, *New Astronomy Reviews* 77, 23–61
- [15] Vedrenne, Gilbert and Atteia, Jean-Luc Gamma-ray bursts: The brightest explosions in the universe;2009
- [16] Turpin, D and Heussaff, V and Dezalay, J-P and Atteia, JL and Klotz, A and Dornic, D Connecting Prompt and Afterglow GRB emission I. Investigating the impact of optical selection effects in the Epi-Eiso plane, *arXiv preprint arXiv:1503.02760*; 2015
- [17] Ghisellini, Gabriele Gamma Ray Bursts: basic facts and ideas, *Proceedings of the International Astronomical Union*;6,(S275),335–343, 2010
- [18] Kumar, Pawan and Zhang, Bing The physics of gamma-ray bursts & relativistic jets, *Physics Reports* ,561;1–109,2015
- [19] Sokolov, VV and Bisnovatyi-Kogan, GS and Kurt, VG and Gnedin, Yu N and Baryshev, Yu V Observational constraints on the angular and spectral distributions of photons in gamma-ray burst sources, *Astronomy reports* ; 50,(8),612–625 ;2006
- [20] Piran, Tsvi Magnetic Fields in Gamma-Ray Bursts: A Short Overview,784,(1),164–174; 2005
- [21] Vergani, Susanna D Studies on the gamma-ray burst phenomenon and on its use to probe the high redshift universe ;Dublin City University;2009
- [22] Pe'Er, Asaf Physics of gamma-ray bursts prompt emission, *Advances in Astronomy* ; (2015) ; 2015

- [23] Selsing, Jonatan Illuminating the dark: with cosmic explosions and their afterglows,*Ph. D. Thesis*; 2018
- [24] Harrison, FA and Bloom, JS and Frail, Dale A and Sari, R and Kulkarni, Shrinivas R and Djorgovski, SG and Axelrod, Tim and Mould, Jeremy and Schmidt, Brian P and Wieringa, Mark H and others. Optical and Radio Observations of the Afterglow from GRB 990510: Evidence for a Jet,*The Astrophysical Journal*,523 (2),L121;1999
- [25] Wijers, RAMJ and Galama, TJ Physical parameters of GRB 970508 and GRB 971214 from their afterglow synchrotron emission,*The Astrophysical Journal*, 523(1) ;177; 1999.
- [26] Costa, E etal and Frontera, F and Heise, J and Feroci, M al and Fiore, F and Cinti, MN and Dal Fiume, D and Nicastro, L and Orlandini, M and Palazzi, E and others, Discovery of an X-ray afterglow associated with the γ -ray burst of 28 February 1997,*Nature* ,387,(6635), 783–785,1997.
- [27] Landauer, Rolf physical nature of information *Physics letters A* ,217, (4-5),188–193 ,1996
- [28] Jacob, Uri and Piran, Tsvi , Neutrinos from gamma-ray bursts as a tool to explore quantum-gravity-induced Lorentz violation,*Nature Physics*,3,(2) ,87..90,2007.
- [29] Rees, MJ and Mészáros, P Relativistic fireballs: energy conversion and time-scales, *Monthly Notices of the Royal Astronomical Society* 258 ,(1), 41P–43P, 1992.
- [30] Mészáros, P and Rees, Martin J Poynting jets from black holes and cosmological gamma-ray bursts, *The Astrophysical Journal*, 482,(1),L29 , 1997.
- [31] Panaitescu, A and Mészáros, P and Rees, MJ Multiwavelength afterglows in gamma-ray bursts: refreshed shock and jet effects,T *The Astrophysical Journal*,503,(1), 314 1998.
- [32] Willingale, R and O'brien, PT and Osborne, JP and Godet, O and Page, KL and Goad, MR and Burrows, DN and Zhang, B and Rol, E and Gehrels, N and others Testing the standard fireball model of gamma-ray bursts using late X-ray afterglows measured by Swift,*The Astrophysical Journal* ,662(2), :1093;,2007.

- [33] Zhang, Bing A burst of new ideas, *Nature* ,444,(7122),1010–1011 ,2006.
- [34] Dermer, Charles D and Mitman, Kurt E Short-timescale variability in the external shock model of gamma-ray bursts ,*The Astrophysical Journal* 513,(1), L5 ,1999.
- [35] Dermer, Charles D Curvature effects in gamma-ray burst colliding shells, *The Astrophysical Journal* , 614 (1),284 2004 .
- [36] Fan, YZ and Wei, DM Late internal-shock model for bright X-ray flares in gamma-ray burst afterglows and GRB 011121 *Monthly Notices of the Royal Astronomical Society: Letters* 34,(1),L42–L46,2005
- [37] Genet, F and Granot, J Realistic analytic model for the prompt and high-latitude emission in GRBs, *Monthly Notices of the Royal Astronomical Society*, 399,(3),1328–1346,2009.
- [38] Fan, Yizhong and Piran, Tsvi Gamma-ray burst efficiency and possible physical processes shaping the early afterglow, *Monthly Notices of the Royal Astronomical Society*,369,(1), 197–206,2006.
- [39] Mangano, Vanessa and La Parola, Valentina and Cusumano, Giancarlo and Mineo, Teresa and Malesani, Daniele and Dyks, Jaroslaw and Campana, Sergio and Capalbi, Milvia and Chincarini, Guido and Giommi, Paolo and others. Swift XRT observations of the afterglow of XRF 050416A, *The Astrophysical Journal*,654,(1),(403),2007
- [40] Ramirez-Ruiz, Enrico and Dray, Lynnette M and Madau, Piero and Tout, Christopher A, Winds from massive stars: implications for the afterglows of γ -ray bursts, *Monthly Notices of the Royal Astronomical Society* ,327,(3),829–840.;2001.
- [41] Birnbaum, Tesla and Zhang, Bing and Zhang, Bin-Bin and Liang, En-Wei Observational constraints on the external shock prior emission hypothesis of gamma-ray bursts, *Monthly Notices of the Royal Astronomical Society*,422,(1), 393–400 ;2012.
- [42] Chevalier, Roger A and Li, Zhi-Yun Wind interaction models for gamma-ray burst afterglows: the case for two types of progenitors *The Astrophysical Journal*,536,(1),195, 2000.

- [43] Granot, Jonathan and Sari, Re'em The shape of spectral breaks in gamma-ray burst afterglows,*The Astrophysical Journal*, 568, (2), 820 ;2002.
- [44] Ghisellini, G and Ghirlanda, G and Nava, L and Firmani, C “Late Prompt” emission in gamma-ray bursts?,*The Astrophysical Journal*, 658, (2), L75, 2007.